Single-particle structures, high-spin isomers, and a strongly coupled band in odd-odd ^{120}Sb

L. Liu (刘雷),[1] S. Y. Wang (王守宇),[1,*] Z. Q. Chen (陈志强),[1] C. Liu (刘晨),[1] B. Qi (亓斌),[1] D. P. Sun (孙大鹏),[1] S. Wang (王硕),[1] Q. An (安强),[1] C. J. Xu (徐长江),[1] P. Zhang (张盼),[1] Z. Q. Li (李志泉),[1] C. Y. Niu (牛晨阳),[1] X. G. Wu (吴晓光),[2] G. S. Li (李广生),[2] C. Y. He (贺创业),[2] Y. Zheng (郑云),[2] C. B. Li (李聪博),[2] S. H. Yao (姚顺和),[2] S. P. Hu (胡世鹏),[2] H. W. Li (李红伟),[2] J. J. Liu (刘嘉健),[2] and J. L. Wang (汪金龙)[2]

[1]*Shandong Provincial Key Laboratory of Optical Astronomy and Solar-Terrestrial Environment, School of Space Science and Physics, Shandong University, Weihai 264209, People's Republic of China*

[2]*China Institute of Atomic Energy, Beijing 102413, People's Republic of China*

(Received 25 November 2013; revised manuscript received 1 April 2014; published 17 July 2014)

Excited states in ^{120}Sb have been investigated using the ^{116}Cd(^{7}Li,3n)^{120}Sb reaction at a beam energy of 34 MeV. A total of 15 new γ rays were added into the level scheme of ^{120}Sb. Most of the observed single-particle states can be interpreted in terms of weak coupling of the odd proton and odd neutron to an excited ^{118}Sn core involving either vibrational states or broken neutron pairs. The previously known strongly coupled rotational band based on the $\pi g_{9/2}^{-1} \otimes \nu h_{11/2}$ configuration has been extended up to the (15^-) state. The configuration-fixed constrained triaxial relativistic mean-field approaches and the particle rotor model are employed to discuss the high-spin isomers and strongly coupled rotational band, respectively.

DOI: 10.1103/PhysRevC.90.014313 PACS number(s): 21.10.Re, 27.60.+j, 23.20.Lv, 21.60.Ev

I. INTRODUCTION

The present work is a part of our systematic study [1–5] of high-spin states with nuclei near the magic number $Z = 50$. Nuclei in this mass region usually exhibit single-particle structures that coexist with collective structures based on proton excitations across the $Z = 50$ shell gap [6–12]. Therefore, these nuclei provide the possibility of studying single-particle and collective effects within the same nuclear system. In addition, some interesting nuclear structure phenomena such as shape evolution, pseudospin doublet bands, and magnetic rotation have also been observed and widely studied in this mass region. In order to explore these systematic properties in heavier nuclei, a standard in-beam γ-ray spectroscopy experiment has been performed to investigate the high-spin states of ^{120}Sb via the ^{116}Cd(^{7}Li,3n)^{120}Sb reaction.

Prior to this work, Vajda *et al.* studied the high-spin states of ^{120}Sb and reported a rotational band in 1983 [13]. The next year, a relatively complete level scheme including single-particle structures was presented in a doctoral thesis [14]. Recently, Moon [15] studied the high-spin states of ^{120}Sb using the ^{120}Sn(^{7}Li,α3n) reaction.

In this article, we report experimental results on high-spin states in ^{120}Sb. The experimental procedure is described in Sec. II. Results and discussion are presented in Sec. III, and conclusions are given in Sec. IV.

II. EXPERIMENTAL PROCEDURE

High-spin states in odd-odd ^{120}Sb were populated via the ^{116}Cd(^{7}Li,3n)^{120}Sb fusion-evaporation reaction with a beam energy of 34 MeV. A self-supporting ^{116}Cd target of 2.5 mg/cm^2 thickness was bombarded with a beam of ^{7}Li from the HI-13 tandem accelerator at the China Institute of Atomic Energy in Beijing. The γ-γ coincidence measurement was carried out using an array consisting of nine Compton-suppressed HPGe detectors, one Compton-suppressed clover detector, and two low-energy photon spectrometer (LEPS) detectors. Approximately 1.1×10^8 γ-γ coincidence events were collected during the experiment. Energy and efficiency calibrations were performed with the standard ^{133}Ba and ^{152}Eu sources. In order to extract the coincidence relationships between γ rays and the multipolarities of the transitions, the coincidence data were sorted off-line into a symmetrized E_γ-E_γ matrix and two asymmetric angular distribution from oriented states (ADO) matrices. The two ADO matrices were constructed using γ rays detected at all angles (y axis) against those detected at $\sim$45° (or $\sim$135°) and $\sim$90° (x axis), respectively. The experimental ADO ratio was calculated by $R_{\mathrm{ADO}}(\gamma) = I_\gamma(at \sim 45°)/I_\gamma(at \sim 90°)$, where the γ-ray intensities were determined in the coincidence spectra gated by γ transitions (on the y axis) of any multipolarity. In the present geometry, by examining the known γ rays in ^{119}Sb [12], the ADO ratios for stretched quadrupole and pure dipole transitions were found to be about 1.4 and 0.7, respectively.

III. RESULTS AND DISCUSSION

The present work confirms most of the previously known levels and transitions in ^{120}Sb [13–15]. In addition, a total of 15 new transitions have been identified and added to the level scheme of ^{120}Sb. The updated level scheme of ^{120}Sb resulting from the present work is illustrated in Fig. 1, and the new transitions are labeled with asterisks. The experimental information on γ rays belonging to ^{120}Sb is listed in Table I. As shown in Fig. 1, all transitions reported in the present work feed eventually to an $I^\pi = 8^-$ isomeric state, which was defined to be the $\pi d_{5/2} \otimes \nu h_{11/2}$ configuration based on magnetic moment measurements [16]. For convenience, the 8^- isomeric state is set as 0 on the energy scale in the present work since the excitation energy of this isomer has not been established.

*sywang@sdu.edu.cn

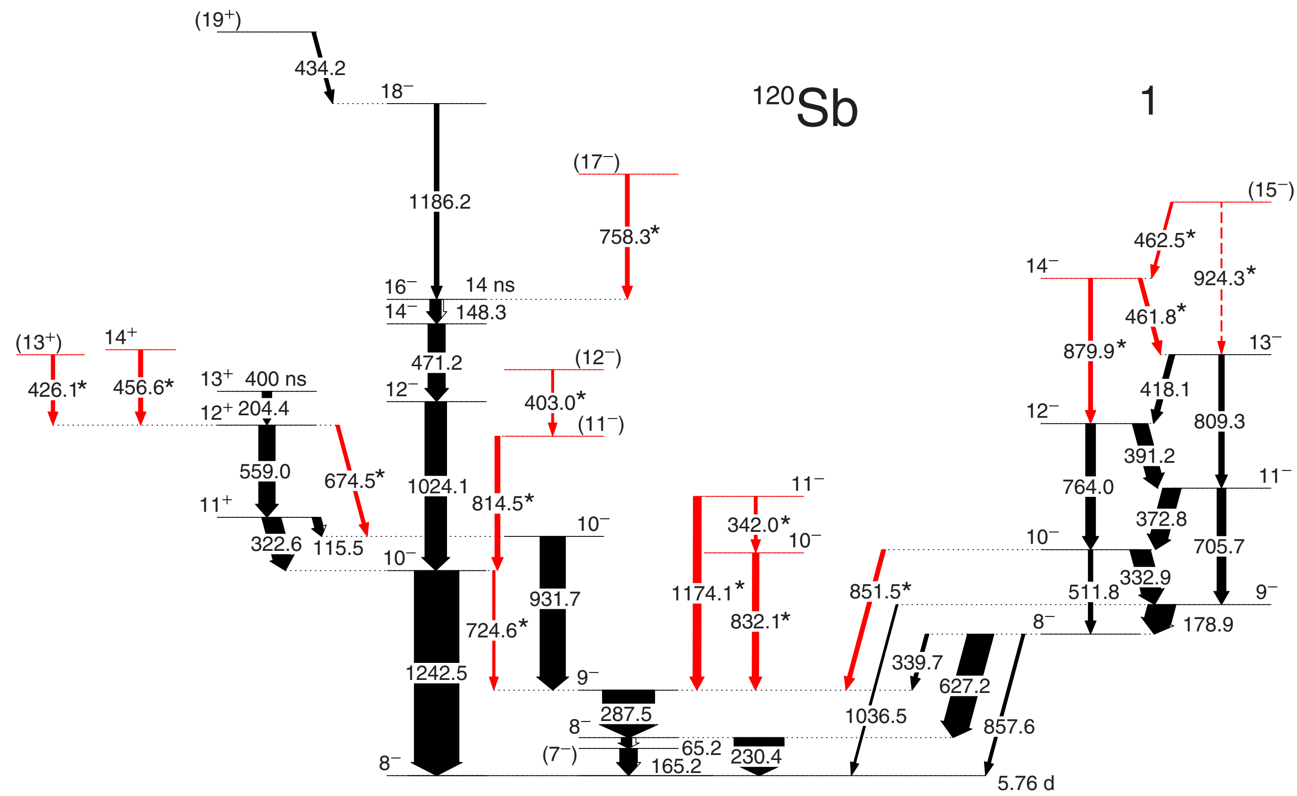

FIG. 1. (Color online) Level scheme of ^{120}Sb deduced from the present work. Transition energies are given in keV, and the widths of the arrows represent the relative intensities of the γ transitions. The level energy of the 8^- isomeric state is set as 0. Newly observed transitions are indicated by asterisks and red lines.

A. Single-particle structures

The left side of Fig. 1 exhibits irregular level structures originating from particle excitations. The present work has added 10 new transitions to the single-particle structures, most of which can be clearly seen in Figs. 2(a) and 2(b). The spins and parities for the known levels were adopted from the previous work [13,14]. For the newly identified levels, spin-parity assignments are deduced from the present measured ADO ratios. It should be noted that, for the four levels that 204.4-, 559.0-, 931.7-, and 287.5-keV transitions depopulate, Ref. [14] assigned these levels as $I^\pi=13^+$, 12^+, 10^-, and 9^-, respectively. While Ref. [15] suggested $I^\pi=(15^+)$, (13^+), (9^+), and (7^+) for the four levels. The present ADO ratios for the four transitions (204.4, 559.0, 931.7, and 287.5 keV) are 0.90(0.28), 1.10(0.16), 1.19(0.08), and 1.22(0.14), respectively. This indicates that these four transitions are of mixed $M1/E2$ character, which is consistent with the assignments in Ref. [14].

To understand the formation of low-lying single-particle states, a systematic comparison of the low-lying single-particle states in ^{120}Sb with those states in its core nuclei ^{119}Sb and ^{118}Sn was made and is shown in Figs. 3(a)–3(c). It can be seen in Figs. 3(a)–3(c) that there is a remarkable similarity between the states. The states shown in ^{119}Sb can be well described in terms of a simple coupling of the valence proton orbitals to the 0_1^+, 2_1^+, and 4_1^+ states in the ^{118}Sn core. Thereby, the indicated states in ^{120}Sb may be attributed to the $h_{11/2}$ valence neutron coupled to the corresponding states in ^{119}Sb. With these features in mind, we propose the 11^+ state in ^{120}Sb to be based on the $\pi h_{11/2} \otimes \nu h_{11/2}$ configuration, and the $I^\pi = (7^-), 8_2^-, 9_1^-$ and 10_2^-, 11_1^- states in ^{120}Sb are members of the $\pi g_{7/2} \otimes \nu h_{11/2} \otimes (^{118}Sn, 0_1^+)$ and $\pi g_{7/2} \otimes \nu h_{11/2} \otimes (^{118}Sn, 2_1^+)$ multiplets, respectively.

As discussed above, the low-lying single-particle states of ^{120}Sb can be well described in terms of the weak-coupling picture. This motivates us to make a weak-coupling interpretation for the high-spin single-particle states in ^{120}Sb. Figure 4 shows a more comprehensive comparison of the single-particle levels in ^{120}Sb with the corresponding levels in the ^{118}Sn core nucleus. As shown in Fig. 4, the level spacings of ^{120}Sb are similar to those of the corresponding ^{118}Sn core. Most of the single-particle states in ^{120}Sb can be explained in terms of coupling the valence proton in the $d_{5/2}$ orbital and the valence neutron in the $h_{11/2}$ orbital to excited spherical states in the ^{118}Sn core. For example, the 8_1^--10_1^--12_2^- sequence in ^{120}Sb is very similar to the 0^+-2^+-4^+ ground-state sequence in the ^{118}Sn core. Therefore, the 8_1^-, 10_1^-, and 12_2^- states in ^{120}Sb can be interpreted as the 0^+-2^+-4^+ sequence in the ^{118}Sn core coupled to the $\pi d_{5/2}$ and $\nu h_{11/2}$ orbitals, which is consistent with the previous assignment for these states [14]. Accordingly, the other states in ^{120}Sb shown in Fig. 4 can also be interpreted in terms of coupling the $\pi d_{5/2}$ and $\nu h_{11/2}$ orbitals to various ^{118}Sn core states. Detailed configuration assignments are exhibited in Fig. 4.

TABLE I. The γ-ray energies, relative intensities, spin-parity assignments, and measured ADO ratios for transitions assigned to ^{120}Sb.

E_γ (keV)	I_γ	$I_i^\pi \to I_f^\pi$	ADO ratio
65.2	21.6(1.8)	$8^- \to (7^-)$	
115.5	16.5(1.7)	$11^+ \to 10^-$	0.72(0.23)
148.3	23.1(2.2)	$16^- \to 14^-$	1.30(0.26)
165.2	34.7(3.0)	$(7^-) \to 8^-$	0.83(0.22)
178.9	53.6(4.3)	$9^- \to 8^-$	0.86(0.19)
204.4	19.1(1.6)	$13^+ \to 12^+$	0.90(0.28)
230.4	100.0	$8^- \to 8^-$	1.49(0.23)
287.5	104.7(5.9)	$9^- \to 8^-$	1.22(0.14)
322.6	37.5(2.2)	$11^+ \to 10^-$	1.04(0.19)
332.9	40.2(2.3)	$10^- \to 9^-$	1.54(0.23)
339.7	9.6(0.8)	$8^- \to 9^-$	1.04(0.12)
342.0	6.1(0.9)	$11^- \to 10^-$	
372.8	36.1(2.1)	$11^- \to 10^-$	1.37(0.25)
391.2	30.5(1.9)	$12^- \to 11^-$	1.42(0.35)
403.0	4.2(0.5)	$(12^-) \to (11^-)$	
418.1	11.4(0.9)	$13^- \to 12^-$	0.84(0.20)
426.1	7.0(0.6)	$(13^+) \to 12^+$	1.23(0.27)
434.2	6.8(0.6)	$(19^+) \to 18^-$	
456.6	8.5(0.8)	$14^+ \to 12^+$	1.50(0.29)
461.8	7.7(0.8)	$14^- \to 13^-$	0.91(0.17)
462.5	5.0(0.7)	$(15^-) \to 14^-$	
471.2	34.7(2.2)	$14^- \to 12^-$	1.63(0.27)
511.8	9.0(0.7)	$10^- \to 8^-$	1.51(0.16)
559.0	33.2(1.3)	$12^+ \to 11^+$	1.10(0.16)
627.2	51.6(2.2)	$8^- \to 8^-$	1.57(0.19)
674.5	6.9(0.6)	$12^+ \to 10^-$	
705.7	17.8(0.4)	$11^- \to 9^-$	1.55(0.20)
724.6	4.8(0.5)	$10^- \to 9^-$	
758.3	8.0(0.6)	$(17^-) \to 16^-$	0.76(0.17)
764.0	19.8(0.8)	$12^- \to 10^-$	1.63(0.37)
809.3	11.1(0.8)	$13^- \to 11^-$	1.67(0.18)
814.5	10.4(1.2)	$(11^-) \to 10^-$	1.12(0.14)
832.1	13.0(1.3)	$10^- \to 9^-$	0.91(0.14)
851.5	8.2(0.6)	$10^- \to 9^-$	0.93(0.13)
857.6	6.0(0.5)	$8^- \to 8^-$	
879.9	8.1(0.6)	$14^- \to 12^-$	1.66(0.30)
924.3	<2.0	$(15^-) \to 13^-$	
931.7	51.2(1.6)	$10^- \to 9^-$	1.19(0.08)
1024.1	43.7(1.1)	$12^- \to 10^-$	1.49(0.16)
1036.5	4.1(0.4)	$9^- \to 8^-$	
1174.1	15.9(0.6)	$11^- \to 9^-$	1.51(0.17)
1186.2	9.5(0.5)	$18^- \to 16^-$	1.46(0.35)
1242.5	90.1(1.7)	$10^- \to 8^-$	1.43(0.14)

In the next step we focus on the single-particle states above the 16^- isomer in ^{120}Sb. As shown in Fig. 4, the 16^- isomer was assigned as the four-particle aligned configuration $\pi d_{5/2} \otimes \nu h_{11/2}^3$, the alignment of a broken pair of neutrons occurring relative to the 8_1^- isomer ($\pi d_{5/2} \otimes \nu h_{11/2}$). Above the 16^- isomer, the excitation spectra are expected to involve a broken neutron pair in the $h_{11/2}$ orbital. On the other hand, as shown in Figs. 3(c) and 3(d), the level structures arising from the 16^- and the 8_1^- isomers are very similar. Therefore, the newly observed (17^-), 18^-, and (19^+) states

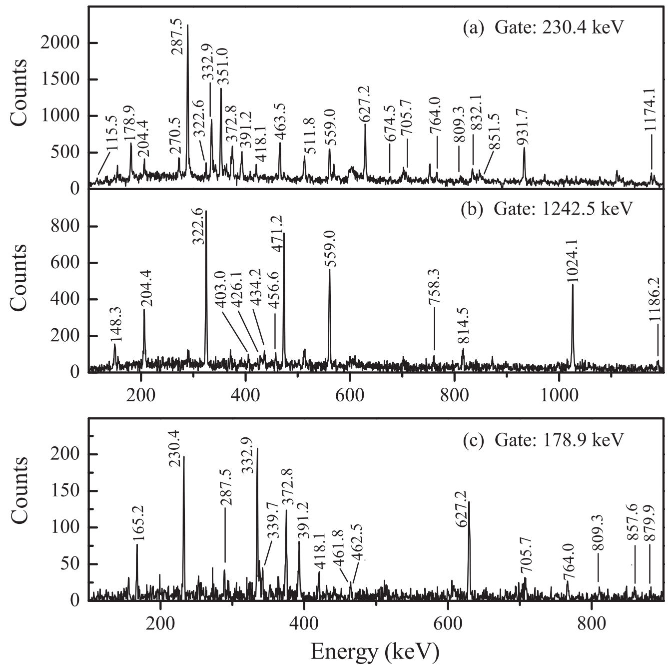

FIG. 2. Representative coincidence spectra gated by the (a) 230.4-keV transition, (b) 1242.5-keV transition, and (c) 178.9-keV transition.

in ^{120}Sb may be associated with the $\nu h_{11/2}^2 \otimes (^{120}Sb, 9_1^-)$, $\nu h_{11/2}^2 \otimes (^{120}Sb, 10_1^-)$, and $\nu h_{11/2}^2 \otimes (^{120}Sb, 11^+)$ configurations, i.e., the $\pi g_{7/2} \otimes \nu h_{11/2}^3$, $\pi d_{5/2} \otimes \nu h_{11/2}^3 \otimes (^{118}Sn, 2_1^+)$, and $\pi h_{11/2} \otimes \nu h_{11/2}^3$ configurations, respectively.

B. High-spin isomers

Nuclear isomers have attracted considerable attention since they may provide a number of applications, such as isomer targets, isomer beams, and the stored energy of isomers [21]. A particular interesting aspect of the present work is the existence of high-spin isomers in the level scheme of ^{120}Sb. The yrast 13^+ and 16^- states have been suggested to be isomers with $T_{1/2} =$ 400 and 14 ns, respectively [14,19]. As Fig. 4 shows, the 13^+ and 16^- isomers have the four-particle aligned configurations $\pi d_{5/2} \otimes \nu h_{11/2}^2 s_{1/2}$ and $\pi d_{5/2} \otimes \nu h_{11/2}^3$, respectively, and they originate from the $\pi d_{5/2}$ and $\nu h_{11/2}$ orbitals coupling to the 5^- and 10_1^+ core states in ^{118}Sn. It should be noted that the 5^- and 10_1^+ states in ^{118}Sn are isomeric [17] and the corresponding 13^+ and 16^- states in ^{120}Sb are isomeric as well. Similarly, we propose that the newly observed 14^+ yrast state in ^{120}Sb is likely to be an isomeric state since the corresponding 7^- core state in ^{118}Sn is an isomeric state with $T_{1/2} = 245$ ns [17]. This is also consistent with the fact that no transitions were observed above the 14^+ state. In order to confirm this hypothesis, the lifetime measurement for the 14^+ state is highly encouraged to be performed.

Configuration-fixed constrained triaxial relativistic mean-field (RMF) approaches [22] were employed for analysis of the high-spin isomers in ^{120}Sb. The RMF calculations show that these high-spin isomers have near-oblate shapes, with

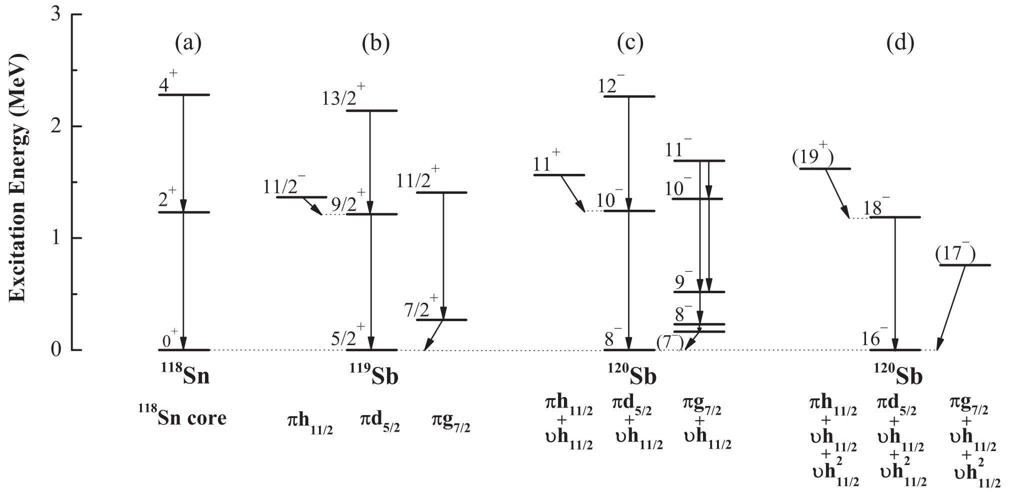

FIG. 3. Systematics of single-particle states in ^{118}Sn [17] and ^{119}Sb [12] compared to the corresponding states in ^{120}Sb.

$\beta_2 = 0.15, \gamma = 55.9^\circ$ for 13_1^+, $\beta_2 = 0.15, \gamma = 59.9^\circ$ for 14^+, and $\beta_2 = 0.17, \gamma = 59.5^\circ$ for 16^-. Although the present RMF calculations cannot distinguish the collective and noncollective oblate shapes, the observation of a number of irregular levels decaying from these isomers indicates that these isomers should be the noncollective oblate where the nuclear symmetry and rotation axes coincide. Such energetically favored noncollective oblate states usually lead to some irregularities in the yrast line, thereby forming the isomeric states [23,24].

C. Strongly coupled band

The right side of Fig. 1 is a strongly coupled rotational band (labeled 1). Band 1 has been interpreted as the $\pi g_{9/2}^{-1} \otimes \nu h_{11/2}$ configuration [13], where the $\pi g_{9/2}$ hole is generated by the proton particle-hole excitation which drives the nucleus to a prolate deformation. Similar bands with the same configuration have been reported in the odd-odd Sb isotopes from $A = 108$ to $A = 120$ [2,4,8–11,13,25–27]. Compared with the lighter odd-odd Sb isotopes, the collective bands

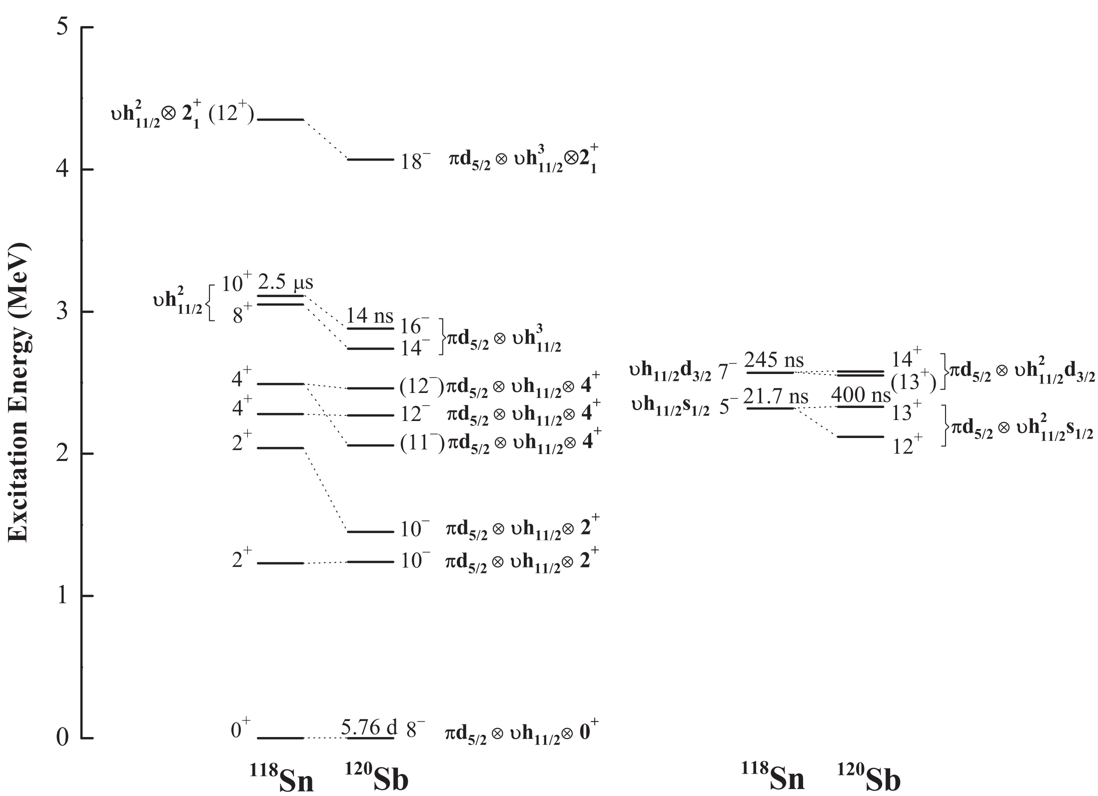

FIG. 4. Comparison of the single-particle levels in ^{120}Sb with the corresponding levels in the ^{118}Sn core nucleus. Levels connected by dashed lines are interpreted as the core states and the corresponding coupled states in terms of weak coupling. Experimental data and configuration assignments for ^{118}Sn are taken from Refs. [17–20].

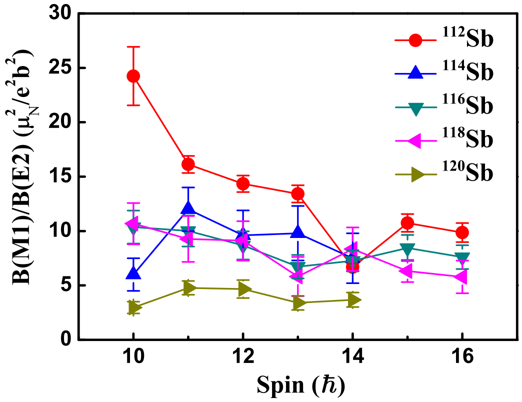

FIG. 5. (Color online) Experimental $B(M1)/B(E2)$ ratios for the $\pi g_{9/2}^{-1} \otimes \nu h_{11/2}$ bands in the odd-odd isotopes ^{112}Sb [8], ^{114}Sb [11], ^{116}Sb [4], ^{118}Sb [2], and ^{120}Sb (present work).

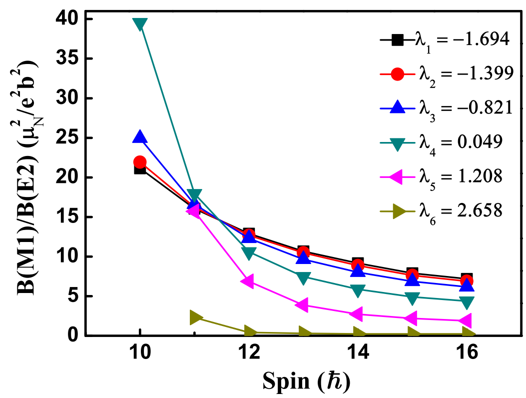

FIG. 6. (Color online) Calculated $B(M1)/B(E2)$ ratios for the $\pi g_{9/2}^{-1} \otimes \nu h_{11/2}$ configuration for different neutron Fermi levels in the $\nu h_{11/2}$ subshell. In the calculations, the odd proton is fixed to be a pure $g_{9/2}$ hole, whereas the odd neutron is treated as a BCS quasiparticle with $\lambda_n = \lambda_1, \lambda_2, \ldots, \lambda_6$, respectively.

with the $\pi g_{9/2}^{-1} \otimes \nu d_{5/2}$ and $\pi g_{9/2}^{-1} \otimes \nu g_{7/2}$ configurations were not observed in ^{120}Sb, which may be ascribed to the lower occupation probability of the $\nu d_{5/2}$ and $\nu g_{7/2}$ valence orbitals as the number of neutrons increases. In the present work, band 1 has been extended up to the (15^-) state by adding two dipole and two quadrupole crossover transitions. In addition, one new linking transition between the lower band member and the single-particle structure is also identified. The sample gated spectra supporting these placements are shown in Figs. 2(a) and 2(c).

Prior to this work, no electromagnetic transition data for the $\pi g_{9/2}^{-1} \otimes \nu h_{11/2}$ band in ^{120}Sb had been reported. The present work has extracted the experimental $B(M1)/B(E2)$ ratios for the $\pi g_{9/2}^{-1} \otimes \nu h_{11/2}$ band in ^{120}Sb from the γ intensities listed in Table I. The extracted $B(M1)/B(E2)$ ratios for the $\pi g_{9/2}^{-1} \otimes \nu h_{11/2}$ band in ^{120}Sb are presented in Fig. 5, together with the corresponding experimental results in the odd-odd isotopes ^{112,114,116,118}Sb [2,4,8,11]. As shown in Fig. 5, the experimental $B(M1)/B(E2)$ ratios exhibit a good systematic feature from ^{112}Sb to ^{120}Sb, i.e., an overall decrease as the neutron number increases. This implies that the different degree of filling of the $\nu h_{11/2}$ subshell probably plays a predominant role in the decrease in experimental $B(M1)/B(E2)$ ratios.

In order to explore the origin of this decrease trend, particle rotor model (PRM) calculations [28,29] were performed. In the PRM calculations, the odd proton is fixed to be a pure $g_{9/2}$ hole, whereas the odd neutron is treated as a BCS quasiparticle and the pairing gap for neutrons is estimated to be 1.1 MeV based on the empirical formula $\Delta = 12/\sqrt{A}$. A common axial symmetrical deformation parameter $\beta_2 = 0.2$ is adopted because the $\pi g_{7/2}$-$\pi g_{9/2}$ level crossing at $\beta_2 \approx 0.2$ stabilizes the nuclear shape [8,9] in the Sb isotopes, thereby the quadrupole moment (Q_0) is taken to be 2.7 eb according to the liquid drop formula. The moment of inertia Im $= 17\ \text{MeV}^{-1}\ \hbar^2$ was taken from Ref. [2]. The g factors for the collective rotor, protons, and neutrons are given by $g_R = Z/A \approx 0.43$, $g_p = 1.261$, and $g_n = -0.209$, respectively. The calculated $B(M1)/B(E2)$ values with configurations of a $\pi g_{9/2}$ proton hole and a quasineutron built on the different neutron Fermi levels (λ_n) in the $\nu h_{11/2}$ subshell are shown in Fig. 6, where λ_n(n = 1, 2 ...,6) corresponds to the quantum number $\Omega(\Omega = \pm\frac{1}{2}, \pm\frac{3}{2}, \ldots, \pm\frac{11}{2})$ in the $\nu h_{11/2}$ subshell [28]. As shown in Fig. 6, the $B(M1)/B(E2)$ ratios exhibit an overall decrease with the neutron Fermi level changing from the bottom (λ_1) to the top (λ_6) of the $\nu h_{11/2}$ intruder subshell, which is consistent with the trend of the experimental $B(M1)/B(E2)$ ratios. Therefore, the decrease in the experimental $B(M1)/B(E2)$ ratios as the neutron number increases may result from the different Fermi level positions of neutrons in the $\nu h_{11/2}$ subshell.

IV. CONCLUSION

The high-spin states in ^{120}Sb have been investigated by in-beam spectroscopy using the ^{116}Cd(^{7}Li,$3n$)^{120}Sb fusion-evaporation reaction at a beam energy of 34 MeV. A total of 15 new γ rays have been added to the level scheme of ^{120}Sb. The RMF and PRM are employed to discuss the high-spin isomers and strongly coupled band, respectively. The results are summarized as follows.

(i) Most of the observed single-particle states can be interpreted in terms of weak coupling of the odd proton and odd neutron to the core states of ^{118}Sn involving either vibrational states or broken neutron pairs.

(ii) Based on the systematic comparison, we propose that the newly observed 14^+ yrast state in ^{120}Sb is likely to be an isomeric state. The RMF calculations are performed for analysis of high-spin isomers in ^{120}Sb, and the calculated results indicate that these isomers have near-oblate shapes.

(iii) The $\pi g_{9/2}^{-1} \otimes \nu h_{11/2}$ band has been extended up to the (15^-) state. A comparison of the experimental $B(M1)/B(E2)$ ratios in odd-odd isotopes $^{112-120}$Sb has been made, exhibiting an overall decrease behavior with increasing neutron number. The PRM calculations indicate that the Fermi level positions of neutrons have a remarkable influence on the $B(M1)/B(E2)$ ratios.

ACKNOWLEDGMENTS

This work was supported by the National Natural Science Foundation (Grant Nos. 11175108 and 11005069), the Independent Innovation Foundation of Shandong University IIFSDU (Grant Nos. 2013ZRYQ001 and 2011ZRYQ004), and the Graduate Innovation Foundation of Shandong University at WeiHai GIFSDUWH (Grant No. yjs11031) of China.

[1] S. Y. Wang *et al.*, Phys. Rev. C **81**, 017301 (2010).
[2] S. Y. Wang *et al.*, Phys. Rev. C **82**, 057303 (2010).
[3] C. Liu *et al.*, Int. J. Mod. Phys. E **20**, 2351 (2011).
[4] S. Y. Wang *et al.*, Phys. Rev. C **86**, 064302 (2012).
[5] C. Liu *et al.*, Phys. Rev. C **88**, 037301 (2013).
[6] D. R. LaFosse, D. B. Fossan, J. R. Hughes, Y. Liang, P. Vaska, M. P. Waring, and J. Y. Zhang, Phys. Rev. Lett. **69**, 1332 (1992).
[7] J. Bron, W. H. A. Hesselink, A. Van Poelgeest, J. J. A. Zalmstra, M. J. Uitzinger, H. Verheul, K. Heyde, M. Waroquier, H. Vincx, and P. Van Isacker, Nucl. Phys. A **318**, 335 (1979).
[8] G. J. Lane *et al.*, Phys. Rev. C **58**, 127 (1998).
[9] E. S. Paul *et al.*, Phys. Rev. C **50**, 2297 (1994).
[10] R. Duffait, J. van Maldeghem, A. Charvet, J. Sau, K. Heyde, A. Emsallem, M. Meyer, R. Beraud, J. Treherne, and J. Genevey, Z. Phys. A **307**, 259 (1982).
[11] P. Van Nes, W. H. A. Hesselink, W. H. Dickhoff, J. J. Van Ruyven, M. J. A. de Voigt, and H. Verheul, Nucl. Phys. A **379**, 35 (1982).
[12] D. R. LaFosse, D. B. Fossan, J. R. Hughes, Y. Liang, H. Schnare, P. Vaska, M. P. Waring, and J.-y. Zhang, Phys. Rev. C **56**, 760 (1997).
[13] S. Vajda, W. F. Piel, Jr., M. A. Quader, W. A. Watson, III, F. C. Yang, and D. B. Fossan, Phys. Rev. C **27**, 2995(R) (1983).
[14] M. A. Quader, Ph.D. thesis, State University of New York at Stony Brook, 1984.
[15] C.-B. Moon, Sae Mulli **60**, 49 (2010).
[16] P. T. Callaghan, M. Shott, and N. J. Stone, Nucl. Phys. A **221**, 1 (1974).
[17] A. van Poelgeest, J. Bron, W. H. A. Hesselink, K. Allaart, J. J. A. Zalmstra, M. J. Uitzinger, and H. Verhuel, Nucl. Phys. A **346**, 70 (1980).
[18] K. Krien, B. Klemme, R. Folle, and E. Bodenstedt, Nucl. Phys. A **228**, 15 (1974).
[19] S. Lunardi, P. J. Daly, F. Soramel, C. Signorini, B. Fornal, G. Fortuna, A. M. Stefanini, R. Broda, W. Meczynski, and J. Blomqvist, Z. Phys. A **328**, 487 (1987).
[20] N. Fotiades, M. Devlin, R. O. Nelson, J. A. Cizewski, R. Krücken, R. M. Clark, P. Fallon, I. Y. Lee, A. O. Macchiavelli, and W. Younes, Phys. Rev. C **84**, 054310 (2011).
[21] P. Walker and G. Dracoulis, Nature (London) **399**, 35 (1999).
[22] J. Meng, J. Peng, S. Q. Zhang, and S. G. Zhou, Phys. Rev. C **73**, 037303 (2006).
[23] A. Bohr and B. R. Mottelson, Phys. Scripta A **10**, 13 (1974).
[24] A. Faessler, M. Ploszajczak, and K. R. S. Devi, Phys. Rev. Lett. **36**, 1028 (1976).
[25] D. G. Jenkins *et al.*, Phys. Rev. C **58**, 2703 (1998).
[26] G. J. Lane *et al.*, Phys. Rev. C **55**, R2127 (1997).
[27] C.-B. Moon, J. U. Kwon, T. Komatsubara, T. Saitoh, N. Hashimoto, J. Lu, H. Kimura, T. Hayakawa, and K. Furuno, Z. Phys. A **357**, 5 (1997).
[28] S. Q. Zhang, B. Qi, S. Y. Wang, and J. Meng, Phys. Rev. C **75**, 044307 (2007); **75**, 024309 (2007); S. Y. Wang, B. Qi, and D. P. Sun, *ibid.* **82**, 027303 (2010).
[29] S. Y. Wang, S. Q. Zhang, B. Qi, J. Peng, J. M. Yao, and J. Meng, Phys. Rev. C **77**, 034314 (2008).